Near-Infrared Absorbing Polymeric Nanoparticles as a Versatile Drug Carrier for Cancer Combination Therapy

*Hua Gong, Liang Cheng, Jian Xiang, Huan Xu, Liangzhu Feng, Xiaoze Shi, and Zhuang Liu**

Poly(3,4-ethylenedioxythiophene):poly(4-styrenesulfonate) (PEDOT:PSS) nanoparticles, after being coated with polyethylene glycol (PEG), are used as a drug carrier to load various types of aromatic therapeutic molecules, including chemotherapy drugs doxorubicin (DOX) and SN38, as well as a photodynamic agent chlorin e6 (Ce6), through π–π stacking and hydrophobic interaction. Interesting functionalities of PEDOT:PSS-PEG as an unique versatile drug delivery platform are discovered. Firstly, for water-insoluble drugs such as SN38, the loading on PEDOT:PSS-PEG dramatically enhances its water solubility, while maintaining its cytotoxicity to cancer cells. Secondly, the delivery of Ce6 by PEDOT:PSS-PEG is able to remarkably accelerate the cellular uptake of Ce6 molecules, and thus offers improved photodynamic therapeutic efficacy. Using DOX-loaded PEDOT:PSS-PEG as the model system, it is demonstrated that the photothermal effect of PEDOT:PSS-PEG can be utilized to promote the delivery of this chemotherapeutic agent, achieving a combined photothermal- and chemotherapy with an obvious synergistic cancer killing effect. Moreover, it is also shown that multiple types of therapeutic agents could be simultaneously loaded on PEDOT:PSS-PEG nanoparticles and delivered into cancer cells. This work highlights the great potential of NIR-absorbing polymeric nanoparticles as multifunctional drug carriers for potential cancer combination therapy with high efficacy.

1. Introduction

The current chemotherapy of cancer suffers greatly by the limited treatment efficacy and severe side effects in patients.[1–3] A variety of strategies, including enhancing the targeting efficiency of drug carriers,[4] increasing the cellular uptake of drugs,[5,6] and developing other therapeutic approaches based on different mechanisms for combined cancer therapy,[7,8] have been actively explored to circumvent these problems. In recent years, photothermal therapy by using nanomaterials absorbing light, particularly near-infrared (NIR) light with superior tissue penetration ability, to generate heat under light exposure, has received tremendous attention.[9–11] The NIR-light-induced phtotothermal heating can not only be used to directly kill cancer cell by hyperthermia, but is also able to remarkably improve the efficacy of other therapeutics under mild heating (e.g., ≈43 °C), by triggering the release of drugs loaded on nanomaterials,[12–14] or enhancing the cellular uptake of drug loaded nanocarriers.[8,15] The combination of photothermal therapy with traditional therapies may be an alternative approach to overcome certain limitations in current cancer treatment, and therefore merits a lot more future research.

However, most photothermal agents adopted currently are inorganic nanomaterials, such as various gold nanostructures and carbon nanomaterials,[16–28] which are usually non-biodegradable and may arouse the long-term toxicity concern because of their long body retention time.[29–32] The development of organic nanoparticles with strong NIR absorbance and the possibility of biodegradation has therefore received significant attention in recent years. A number of NIR-absorbing organic conductive polymers, such as polypyrrole,[33–35] polyaniline,[36] and poly(3,4-ethylenedioxythiophene):poly(4-styrenesulfonate) (PEDOT:PSS)[37] have emerged as a new type of photothermal agent, showing encouraging cancer treatment efficacy in a number of animal experiments. It has also been reported that water soluble conjugated polymers can be used as drug carriers to load drugs such as DOX and porphyrin.[38–40] Therefore, we wonder whether these organic NIR-absorbing nanoparticles could be used for drug delivery and cancer combination therapy, which has not yet been reported to our best knowledge.

In our previous study, we found that organic nanoparticles based on polyethylene glycol (PEG) coated PEDOT:PSS, a conjugated polymer with strong NIR absorbance, showed rather high passive tumor accumulation owing to the enhanced permeability and retention (EPR) effect of cancerous tumors, and could serve as a powerful photothermal agent with excellent tumor ablation effect under NIR laser irradiation, in our mouse tumor model experiments. Importantly, no appreciable

H. Gong, L. Cheng, J. Xiang, H. Xu, L. Z. Feng, X. Z. Shi, Prof. Z. Liu
Jiangsu Key Laboratory for Carbon-Based Functional Materials & Devices
Institute of Functional Nano & Soft Materials Laboratory (FUNSOM)
Soochow University
Suzhou, Jiangsu, 215123, China
E-mail: zliu@suda.edu.cn

DOI: 10.1002/adfm.201301555

toxicity of PEDOT:PSS-PEG nanoparticle was found in our in vitro cell culture assays and in vivo animal experiments, as evidenced by both histology and hematology data.[37] Therefore, in this work, we want to test if the same type of conjugated polymeric nanoparticles, PEDOT:PSS-PEG, could be used as a drug carrier for combined cancer combination therapy. Interestingly, we find that a number of therapeutic molecules with aromatic structures, including a water-soluble anti-cancer drug doxorubicin (DOX), a water-insoluble drug SN38 (a camptothecin derivative), and a photosensitizer chlorine 6(Ce6), could all be effectively loaded on PEDOT:PSS-PEG nanoparticles with good stability and high loading capacity. It is speculated that the aromatic drug loading behaviors in our conjugated polymer system could be similar to that on carbon nanotubes and graphene with delocalized π-electrons.[41,42] More importantly, loading of those therapeutics on PEDOT:PSS-PEG has a number of unique benefits, including improving water-solubility for the water-insoluble drug, accelerating cellular uptake of the photosensitizer for enhanced efficacy in photodynamic therapy, enabling combined photothermal- and chemotherapy for synergistic cancer cell killing, as well as allowing for co-loading and co-delivery of multiple therapeutic molecules simultaneously. Our work presents a novel type of drug carrier based on NIR-absorbing organic nanoparticles with a number of different functionalities, which could be integrated together in future studies to develop new cancer treatment approaches.

2. Results and Discussion

2.1. Loading of Therapeutics on PEDOT:PSS-PEG Nanoparticles

PEDOT:PSS-PEG nanoparticles were prepared from commercial PEDOT:PSS polymeric nanoparticles via layer-by-layer assembly of charged polymers and subsequent PEGylation, following our previously established protocol.[37] The obtained PEDOT:PSS-PEG nanoparticles were in a dark blue color, and showed great stability in various physiological solutions. Detailed preparation procedure and characterization data of PEDOT:PSS-PEG have been described in our previous report.[37]

A large number of previous studies have uncovered that nano-surfaces with delocalized π-electrons, such as that of carbon nanotubes and graphene, are able to adsorb aromatic molecules via π–π stacking and hydrophobic interaction, enabling efficient loading of various aromatic drug molecules.[42,43] Since PEDOT is also a conjugated polymer with delocalized π-electrons,[44] we thus wondered whether our PEDOT:PSS-PEG could also serve as a nanocarrier to load aromatic therapeutic molecules for drug delivery. Three types of aromatic molecules including two anticancer drugs DOX (water-soluble) and SN38 (water-insoluble), as well as a photosensitizer Ce6, widely used for photodynamic therapy, were chosen in our experiments (**Figure 1**a). The loading of DOX, Ce6, and SN38 was conducted in pH 8.0 phosphate buffer, pH 7.4 phosphate buffer, and a mixture of water and dimethylsulfoxide (DMSO) (10%), respectively (see the Experimental Section for details). After removal of excess drug molecules, the purified drug loaded samples including PEDOT:PSS-PEG-DOX, PEDOT:PSS-PEG-SN38, and PEDOT:PSS-PEG-Ce6 were measured by UV-VIS-NIR absorbance spectroscopy. Encouragingly, all three types of molecules were effectively loaded on PEDOT:PSS-PEG nanoparticles, showing concentration-dependent loading capabilities (Figure 1b–g). The maximal drug loading capacities (weight ratios between the drug and PEDOT) were determined to be ≈100% for DOX, ≈40% for Ce6, and ≈80% for SN38. Above those loading concentrations, the drug loading capacity became saturated (for Ce6 and SN38), or the drug loaded complex became unstable (for DOX). Nevertheless, the rather high loading capacities achieved here suggest the high efficiency of using PEDOT:PSS-PEG as a novel drug carrier for a variety of different therapeutic molecules.

We next tested the morphology and stability of three different drug loaded polymeric nanoparticles. Dynamic light scattering (DLS) data (Figure 1h) showed that the loading of drugs did not significantly affect the overall size of PEDOT:PSS-PEG nanoparticles, and the average diameters of PEDOT:PSS-PEG, PEDOT:PSS-PEG-DOX, PEDOT:PSS-PEG-SN38, and PEDOT:PSS-PEG-Ce6 were measured to be about 141.9 ± 9.4 nm, 155.3 ± 12.5 nm, 149.7 ± 11.0 nm, and 139.3 ± 8.3 nm, respectively. The atomic force microscopy (AFM) images (Supporting Information, Figure S1) also revealed that PEDOT:PSS-PEG nanoparticles before and after different drug loadings exhibited similar sizes without noticeable aggregation, although the AFM measured diameters of nanoparticles in the dried form on a rigid substrate might not accurately reflect their hydrodynamic sizes in aqueous solutions. Furthermore, the scanning electron microscope (SEM) images (Supporting Information, Figure S2) showed the surface structure didn't change significantly after loading of the three drugs.

One basic requirement for a usable drug delivery nanocarrier is that it should be highly stable in physiological environments containing high concentrations of salts and proteins. In our experiments, we uncovered that PEDOT:PSS-PEG loaded with three different therapeutic molecules at their respective maximal loadings showed excellent stability in various physiologic solutions, without showing any agglomeration in phosphate buffered saline (PBS), serum-containing RPMI-1640 cell medium, and fetal bovine serum (FBS) (Figure 1i). It worth mention that SN38 itself is highly water-insoluble, making it impossible to be directly used in the clinic.[45] Loading of SN38 on PEDOT:PSS-PEG dramatically enhances the water solubility of this drug to be up to ≈1.6 mg mL^{-1}, which is a remarkable advantage of our drug delivery system.

Drug release experiments under different pH conditions were conducted to investigate the drug release profiles of the three drug-loading systems. From Supporting Information, Figure S5a–c, PEDOT:PSS-PEG-Ce6 and PEDOT:PSS-PEG-SN38 were stable in both pH 7.4 and pH 5.0 buffers without significant drug release within 24 h. In contrast, an obvious pH-dependent drug release behavior was observed for PEDOT:PSS-PEG-DOX, which showed much accelerated DOX release under the acidic pH at 5.0. This phenomenon is probably due to the protonation of the amino group in the DOX molecule, which weakens the interaction between PEDOT and DOX by generating a positive charge on the DOX molecule.

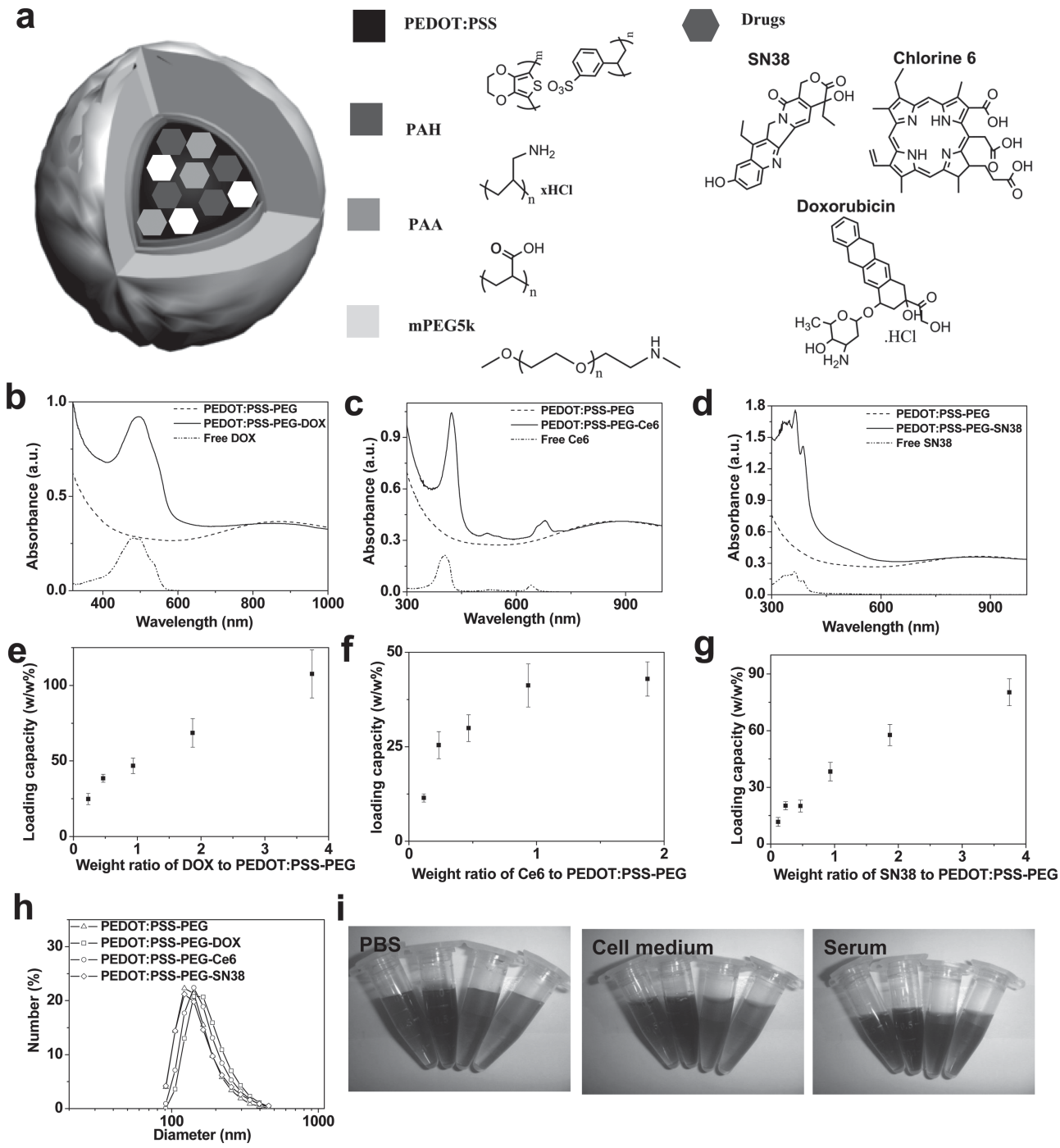

Figure 1. Loading of therapeutic molecules on PEDOT:PSS-PEG. a) A schematic drawing showing DOX, Ce6, and SN38 loaded on PEDOT:PSS-PEG. b–d) UV-vis-NIR spectra of PEDOT:PSS-PEG-DOX, PEDOT:PSS-PEG-Ce6, and PEDOT:PSS-PEG-SN38 with various drug loading concentrations. e–f) The drug loading capacities in three drug loaded PEDOT:PSS-PEG systems as the function of feeding drug concentrations. h) Hydrodynamic diameters of PEDOT:PSS-PEG, PEDOT:PSS-PEG-DOX, PEDOT:PSS-PEG-Ce6, and PEDOT:PSS-PEG-SN38. i) Photos showing PEDOT:PSS-PEG, PEDOT:PSS-PEG-DOX, PEDOT:PSS-PEG-Ce6, and PEDOT:PSS-SN38 (from left to right) in PBS, cell medium, and serum after 24 h of incubation.

2.2. PEDOT:PSS-PEG Nanoparticles for the Delivery of Chemotherapy

Our previous study evidenced that although PEDOT:PSS before PEG coating exhibited certain toxicity to cells at high concentrations, PEDOT:PSS-PEG after PEGylation was not toxic to cells, and more importantly rendered no appreciably toxicity to the treated animals such mice at the tested dose. In this study, we also found that bare PEDOT:PSS-PEG without drug loading showed no obvious toxicity to 4T1 cells (Supporting Information, Figure S3).

To see if therapeutic molecules loaded on PEDOT:PSS-PEG were still effective, we firstly examined the cytotoxicity of PEDOT:PSS-PEG-DOX and PEDOT:PSS-PEG-SN38 towards 4T1 cells, in comparison to free drugs. **Figure 2**a,b shows the half maximum inhibitory concentration (IC50) of PEDOT:PSS-PEG-DOX to 4T1 cells after 48 h of incubation was measured to be about ≈3.2 μM, while that of free DOX was ≈0.7 μM. Similar to many other drug delivery systems, the slightly reduced in vitro cell toxicity of PEDOT:PSS-PEG-DOX in comparison to free DOX is not surprising and likely due to the fact that DOX molecules have to be released from the carrier to be effective, and this release process happens gradually.

SN38 as a camptothecin analogue is a potent topoisomerase I inhibitor. Despite its strong cancer cell killing efficacy, SN38 has rather poor water-solubility and cannot be directly administrated into patients. Irinotecan, also named as CPT-11, is a water-soluble prodrug for SN38, and has been approved by the US Food and Drug Administration (FDA) for cancer treatment.[46] In our experiments with 4T1 cells, both the water soluble PEDOT:PSS-PEG-SN38 and free SN38 dissolved in DMSO showed similar IC50 values at ≈1.2 μM, which was much lower than that of CPT11 (IC50 ≈17 μM). The remarkably enhanced water solubility with retained cytotoxicity of PEDOT:PSS-PEG-SN38 present the advantage of our drug delivery system for water-insoluble drugs.

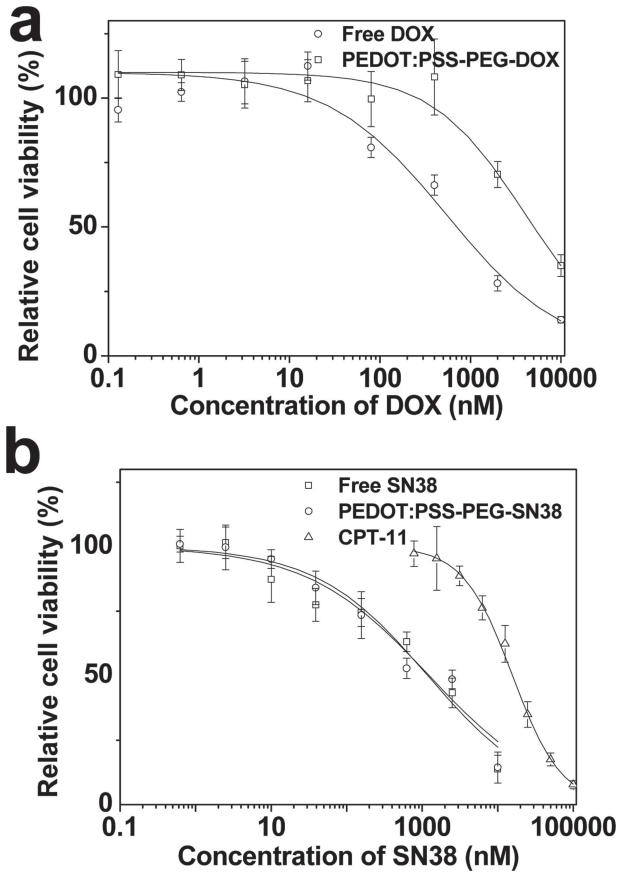

Figure 2. In vitro cell viability test. a) Relative viabilities of 4T1 cells after incubation with various concentrations of free DOX and PEDOT:PSS-PEG-DOX for 48 h. b) Relative viabilities of 4T1 cells after incubation with various concentrations of free SN38 and PEDOT:PSS-PEG-SN38 for 48 h. The water-insoluble SN38 was pre-dissolved in DMSO and diluted by PBS before being added into cell cultures. Error bars are based on triplicated samples.

2.3. PEDOT:PSS-PEG Nanoparticles for the Delivery of Photodynamic Therapy

Photodynamic therapy (PDT) as a promising way for tumor treatment relies on the singlet oxygen ($^1O_2$) produced by photosensitizer (PS) molecules under light irradiation at the appropriate wavelength. However, the limited lifetime and low diffusion rate of $^1O_2$ require the cell internalization of PS molecules to achieve the optimal effect.[8,47] Various nanocarriers have been developed to increase the water solubility of PS molecules and enhance their cellular uptake.[48] We thus wondered whether PEDOT:PSS-PEG-Ce6 nanoparticles developed in our work would offer any significant advantage in the delivery of PDT.

Firstly, we measured the $^1O_2$ production by a singlet oxygen sensor green (SOSG), whose fluorescence would increase in the presence of $^1O_2$. It was found that the $^1O_2$ generation by PEDOT:PSS-PEG-Ce6 decreased by a half in comparison to free Ce6 (Supporting Information, Figure S6), likely due to the direct contact between Ce6 and PEDOT that partially quenched the light-induced $^1O_2$ generation, consistent to the quenching of Ce6 fluorescence after loading on PEDOT:PSS-PEG nanoparticles (Supporting Information, Figure S4b).

Next, we studied the in vitro photodynamic cancer cell killing efficiencies of Ce6 loaded PEDOT:PSS-PEG. **Figure 3**a shows the relative viabilities of 4T1 cells after being exposed to the 660 nm laser (0.1 W cm^{-2}, 10 min) as a function of equivalent Ce6 concentrations. It was found that PEDOT:PSS-PEG-Ce6, which showed no appreciable dark toxicity, was much more toxic than free Ce6 under laser irradiation. Considering the reduced singlet oxygen generation ability for PEDOT:PSS-PEG-Ce6, we speculated that our Ce6-carrying nanoparticles would exhibit accelerated cellular uptake compared with free Ce6 molecules. In order to prove this hypothesis, we carefully studied the cellular uptake behaviors of Ce6-loaded nanoparticles in comparison to free Ce6. Confocal fluorescence imaging of cells (Figure 3b) uncovered that the Ce6 fluorescence inside cells incubated with PEDOT:PSS-PEG-Ce6 was much stronger than those treated with free Ce6, even though the fluorescence of Ce6 in the former formation was partially quenched due to its loading on PEDOT:PSS-PEG (Supporting Information, Figure S4b). To quantitatively determine the cellular uptake of Ce6, we extracted the Ce6 molecules from cell lysate samples following the Ogura procedure.[49] Ce6 molecules loaded on PEDOT:PSS-PEG were completely detached after the strong base treatment as indicated by the ≈100% fluorescent recovery, likely owing to the deprotonation of carboxyl group of Ce6 molecules under the basic condition. Ce6 extraction data (Figure 3c) further confirmed that the cellular uptake of Ce6 in PEDOT:PSS-PEG-Ce6 incubated cells was 5.6- and 5.8-fold higher than cells treated with free Ce6, after 2 and 6 h of incubation, respectively. Therefore, we conclude that our PEDOT:PSS-PEG nanocarrier could

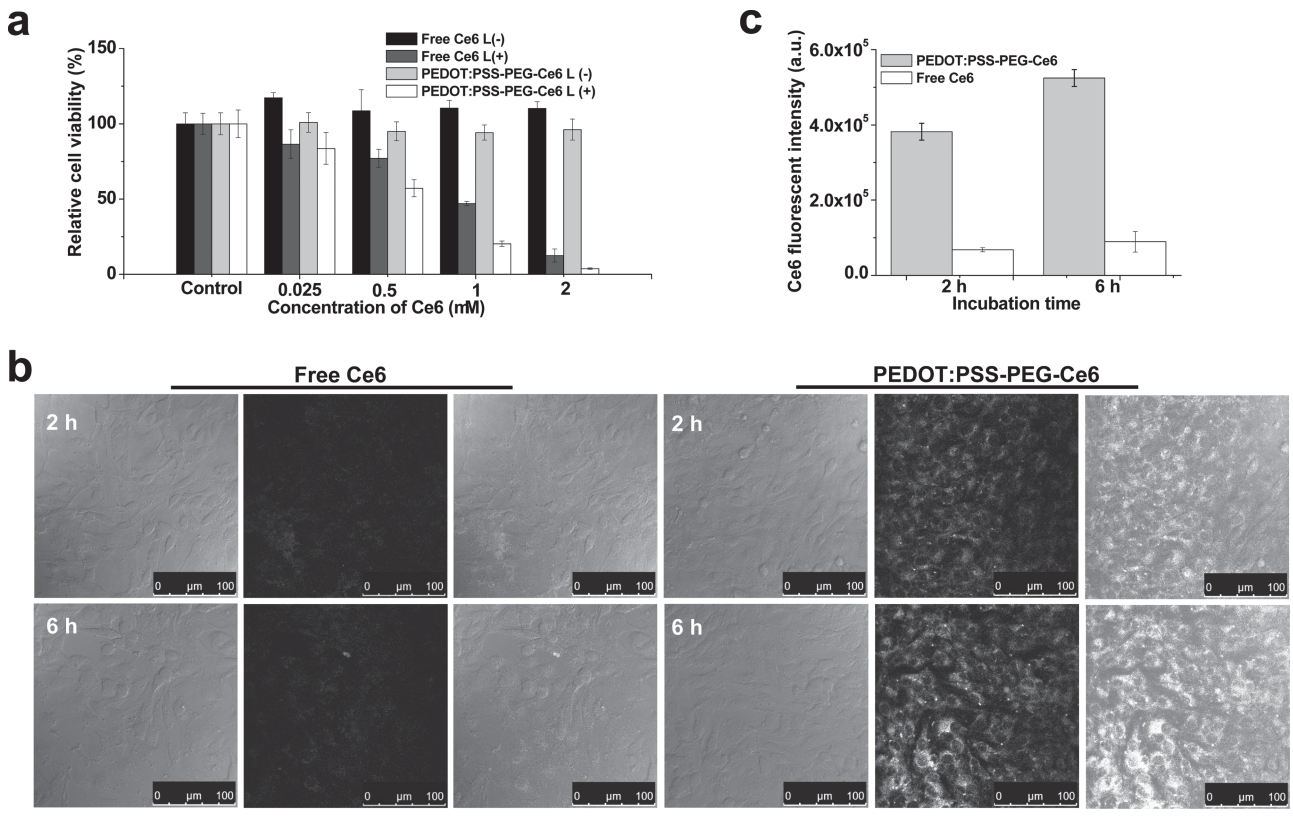

Figure 3. Delivery of photodynamic therapy. a) Photodynamic cancer cell killing. 4T1 cells were incubated with various concentrations of Ce6 or PEDOT:PSS-PEG-Ce6 for 6 h and then exposed to the 660 nm laser at a power density of 0.1 W cm^{-2} for 10 min. Cells without laser irradiation were used as the control. Error bars are based on standard deviations of 4 parallel samples. *P* values: * $p < 0.01$. b) Confocal fluorescence images of 4T1 cells incubated with free Ce6 or PEDOT:PSS-PEG-Ce6 (2 μM Ce6) for 2 or 6 h. c) Quantitative Ce6 cellular uptake measurement determined by Ce6 fluorescence intensities of the cell lysates for samples in (b).

remarkably promote the intracellular shuttling of PS molecules such as Ce6, to improve the photodynamic therapeutic efficacy.

2.4. Photothermally Enhanced Chemotherapy

It has been reported that mild heating can greatly enhance cellular uptake of nanomaterials due to the increased cell membrane mobility at a temperature (e.g., 43 °C) slightly above the physiological temperature.[15,50–52] Since PEDOT:PSS-PEG has already been proven to be a powerful photothermal agent (**Figure 4**b), we wondered whether the photothermal effect of this NIR-absorbing nanocarrier could be utilized to accelerate the endocytosis process of PEDOT:PSS-PEG-DOX and enhance the chemotherapeutic efficacy (Figure 4a).

Cells were incubated with free DOX, PEDOT:PSS-PEG-DOX at the equivalent DOX concentration. While one group of cells was immediately irradiated by an 808 nm laser at the power density of 0.15 W cm^{-2} for 20 min, the other group was left in dark. After irradiation, cells were washed with PBS three times, to remove the excess materials. Both confocal fluorescence images and flow cytometry data uncovered that, while DOX incubated cells with or without laser irradiation showed similar levels of DOX fluorescence, the DOX fluorescence in PEDOT:PSS-PEG-DOX treated cells could be remarkably enhanced by laser irradiation, and was higher than that in cells incubated with DOX, despite the significant quenching of DOX fluorescence after loading on nanoparticles (Supporting Information, Figure S4a). To further confirm that the increased DOX fluorescence upon laser irradiation was indeed resulted from the photothermally enhanced intracellular drug delivery, cells after various treatments were solubilized by a lysis buffer with DOX extracted by a HCl/isopropanol solution, which could allow complete detaching of DOX molecules from PEDOT:PSS-PEG nanoparticles. Quantitative measurement of intracellular DOX levels revealed that the DOX uptake of PEDOT:PSS-PEG-DOX increased by as much as 5.1-fold after laser exposure (Figure 4e). Those result suggest that the photothermal effect of PEDOT:PSS-PEG could be utilized to accelerate the cellular uptake of chemotherapeutic agents for remotely controlled drug delivery and combined cancer therapy.

Then, we wondered whether the photothermal effect of PEDOT:PSS-PEG and chemotherapeutic effect of DOX could be combined together to realize a synergistic effect in cancer cell killing. 4T1 cells were treated by free DOX, PEDOT:PSS-PEG, and PEDOT:PSS-PEG-DOX for 20 min, with or without laser irradiation at different power densities. After removal of excess reagents, cells were re-incubated in fresh cell medium

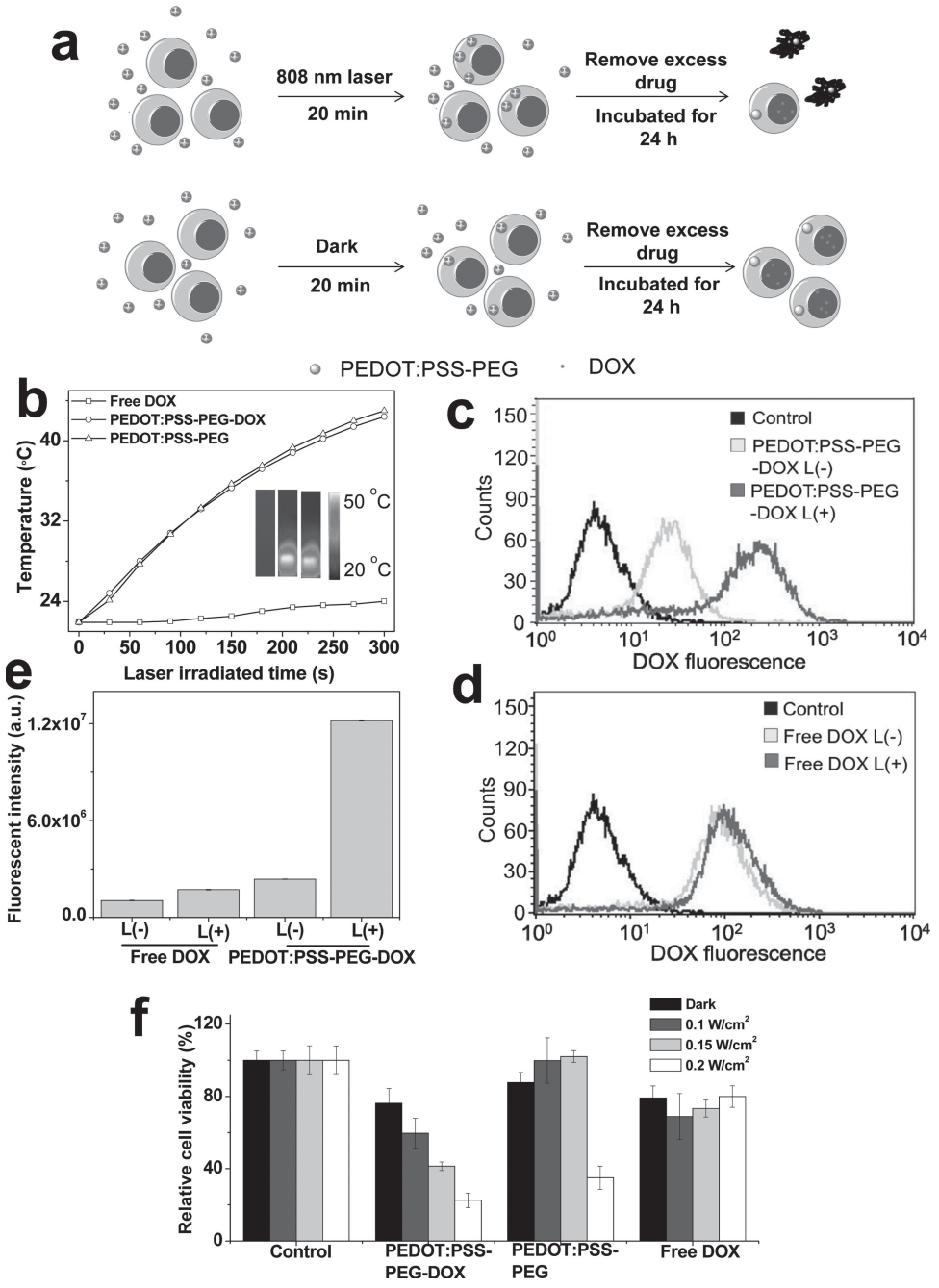

Figure 4. Photothermally enhanced chemotherapy. a) A scheme showing photothermally enhanced cellular uptake of PEDOT:PSS-PEG-DOX. b) Temperature elevation curves of free DOX, PEDOT:PSS-PEG-DOX, and PEDOT:PSS-PEG solutions exposed to the 808 nm laser at the power density of 0.25 W cm^{-2}. Inset: IR thermal images of the three different samples after laser irradiation for 5 min. c,d) Flow cytometry measurement of cellular DOX fluorescence for cells incubated with c) PEDOT:PSS-PEG-DOX or d) free DOX, with or without laser irradiation (808 nm, 0.15 W cm^{-2}, 20 min). e) DOX fluorescent intensities of cell lysates for samples in (c,d). f) Relative viabilities of 4T1 cells after various treatments indicated. The MTT assay was conducted 24 h after incubation and laser irradiation.

for 24 h before their relative viabilities were determined. While free DOX at our experimental conditions only showed a low level of toxicity which was independent from laser irradiation, cells incubated with PEDOT:PSS-PEG-DOX (at the same DOX equivalent concentration) showed greatly decreased viabilities at the increase of 808 nm laser power densities from 0.1 to 0.2 W cm^{-2} (Figure 4f). As for plain PEDOT:PSS-PEG without DOX loading, its direct photothermal effect would not significantly induce cell death at laser power densities at 0.1 and 0.15 W cm^{-2}. Under a high power density at 0.2 W cm^{-2}, the photothermal effect of plain PEDOT:PSS-PEG resulted in significant cell killing, which, however, was still less effective

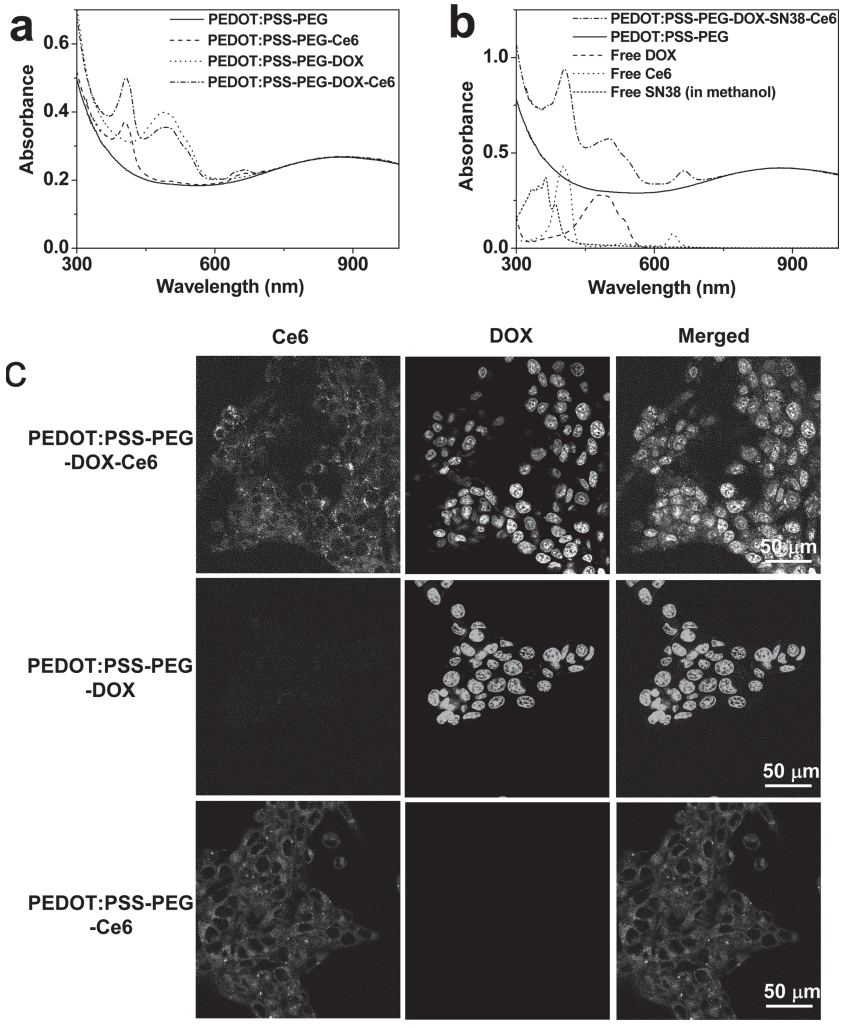

Figure 5. Co-loading of therapeutic molecules on PEDOT:PSS-PEG. a) UV-vis-NIR spectra of PEDOT:PSS-PEG, PEDOT:PSS-PEG-Ce6, PEDOT:PSS-PEG-DOX, and PEDOT:PSS- PEG-DOX-Ce6. b) UV-vis-NIR spectra of PEDOT:PSS-PEG-DOX-SN38-Ce6, PEDOT:PSS-PEG, free DOX, free Ce6, and free SN38 (in methanol). c) Confocal fluorescence images of 4T1 cells incubated with PEDOT:PSS-PEG-DOX-Ce6, PEDOT:PSS-PEG-DOX, and PEDOT:PSS-PEG-Ce6 at equivalent drug concentrations ([DOX] = 12 mM, [Ce6] = 10 mM). Green and red colors indicated Ce6 and DOX fluorescence recorded under 633 nm and 488 nm excitations, respectively.

than the combined photothermal- and chemotherapy delivered by PEDOT:PSS-PEG-DOX. Our results collectively demonstrate that the mild photothermal heating could remarkably enhance the efficacy of chemotherapy by promoting the cellular uptake of drug molecules, realizing a synergistic effect in the cancer combination therapy.

2.5. Co-Loading and Co-Delivery of Therapeutics

In consideration of the successful loading of individual drug molecules on PEDOT:PSS-PEG, at last, we wondered whether different therapeutic agents could be packed together in a single drug carrier system simultaneously. Indeed, **Figure 5**a shows that DOX and Ce6 could be co-loaded on PEDOT:PSS-PEG, according to the characteristic absorbance peaks for each drug. Figure 5b further demonstrates all three types of drug molecules, DOX, Ce6, and SN38 could be co-loaded on PEDOT:PSS-PEG nanoparticles, at the individual loading capacities at 35.3%, 43.6%, and 26.9%, respectively, as determined by spectral deconvolution of the absorbance spectrum of PEDOT:PSS-PEG-DOX-SN38-Ce6. In order to study the intracellular delivery behaviors of our multiple drug co-loaded system, we monitored the fluorescence of DOX and Ce6 in cells after 6 h of incubation with PEDOT:PSS-PEG-DOX-Ce6, PEDOT:PSS-PEG-DOX, and PEDOT:PSS-PEG-Ce6. Confocal fluorescence images (Figure 5c) show that the DOX fluorescence (red color) mainly accumulated in the nuclei of PEDOT:PSS-PEG-DOX incubated cells, likely due to the pH-induced DOX release from the nanocarriers located inside cell lysosomes, and the fact that the fluorescence of unreleased DOX retained on nanoparticles was largely quenched, while Ce6 fluorescence (green color) mainly accumulated in the cytoplasm of cells incubated PEDOT:PSS-PEG-Ce6. Our data suggest that both types of therapeutic molecules could simultaneously delivered into cells by our multifunctional nanocarrier, promising for potential applications in cancer combination therapy.

3. Conclusions

We uncovered that NIR-absorbing conjugated polymers, such as PEDOT:PSS in this case, with appropriate surface coating (e.g., PEGylation), could serve as a versatile drug delivery platform with a number of interesting advantages. Aromatic therapeutic molecules, even including water-insoluble drugs such as SN38, can be effectively loaded on those PEDOT:PSS-PEG nanoparticles with high loading capacity, obtaining drug loaded nanoparticles with high water solubility, excellent physiological stability, and retained therapeutic efficiency. As for the delivery of photodynamic agent, loading of Ce6 on PEDOT:PSS-PEG could remarkably enhance the cellular uptake of this PS molecule, resulting in dramatically improved photodynamic cancer cell-killing efficiency. Using DOX loaded nanoparticles as the model system, we further demonstrate that the photothermal effect of PEDOT:PSS-PEG-DOX could be utilized to promote the delivery of chemotherapeutic agent, and thus to realize the combined cancer therapy with an obvious synergistic effect. Moreover, multiple types of therapeutic molecules can be simultaneously co-loaded on PEDOT:PSS-PEG nanoparticles, for potential applications in combined chemo-, photodynamic, and photothermal therapy of cancer. Our results demonstrate for the first time the great promise of using NIR-absorbing

conjugated polymers as a novel class of multifunctional drug carrier, and encourage further exploration of those polymeric nanoparticle systems for cancer combination therapy.

4. Experimental Section

Synthesis of PEDOT:PSS-PEG: PEDOT:PSS (CLEVIOS PH1000) was purchased from Baier Chemical Industrial Co. PEGylated PEDOT:PSS was synthesized according to the protocol previously reported by our lab with slightly modifications.[37] Firstly, the newly purchased PEDOT:PSS was dialyzed through 3.5 kDa molecular weight cut-off (MWCO) dialysis membrane to remove salts. 5 mL PEDOT:PSS solution (2.14 mg mL^{-1}) was then dropwisely added to 10 mL poly(allylamine hydrochloride) (PAH) solution (M_w = 15 000, 2 mg mL^{-1}) under ultrasonication. After stirring for 6 h at room temperature, the above solution was purified by ultra-filtration filters (Millipore, MWCO = 100 kDa) to remove excess PAH. The obtained PEDOT:PSS/PAH solution was then dropwisely added to 10 mL poly(acrylic acid) (PAA solution) (M_w = 1800, 2 mg mL^{-1}) under ultrasonication, stirred for 3 h, and then purified through ultra-filtration filters (MWCO = 100 kDa). After adjusting the pH of the above solution to 7.4, 5 mg of N-(3-dimethylaminopropyl-N′-ethylcarbodiimide) hydrochloride (EDC, Fluka Inc.) was added to induce the crosslink between PAH and PAA layers coated on PEDOT:PSS. Finally, 5 mL of PEDOT:PSS/PAH/PAA solution at the concentration of 2 mg mL^{-1} were mixed with 30 mg mPEG-5K-NH_2 under ultrasonication for 30 min before 10 mg EDC were added. After overnight reaction, the prepared PEDOT:PSS-PEG was purified by ultra-filtration filters (MWCO = 100 kDa) and stored at 4 °C until use.

Loading of DOX, Ce6, and SN38 on PEDOT:PSS-PEG: For DOX loading, the PEDOT:PSS-PEG solution (final concentration = 0.04 mg mL^{-1}) was mixed with DOX at various concentrations at pH 8.0 overnight under stirring. Excess unbound DOX was removed by ultra-filtration (MWCO = 100 kDa) and repeated water washing. Ce6 loading and purification was conducted by using the same protocol, except that Ce6 was dissolved in DMSO before being added into PEDOT:PSS-PEG, and the loading pH was 7.4 instead of 8.0. The obtained PEDOT:PSS-PEG-DOX and PEDOT:PSS-PEG-Ce6 samples were stored under 4 °C until use.

For the loading of SN38, various volumes of SN38 dissolved in DMSO (4 mg mL^{-1}) was added into the PEDOT:PSS-PEG solution (final concentration = 0.04 mg mL^{-1}) under ultrasonication to get a clear solution, which was stirred for overnight. For purification, the majority of un-loaded free SN38 was precipitated and removed by centrifugation at 5000 rpm for 5 min, obtaining a clear supernatant which was further purified by ultra-filtration (MWCO = 100 kDa) and repeated water washing. The obtained PEDOT:PSS-PEG-SN38 was also stored under 4 °C until use.

Characterization: Atomic force microscopy (AFM) images were taken by MultiMode V atomic force microscopy (Veeco, USA). The sizes of nanoparticles were measured using ZEN3690 zetasizer (Malvern, USA). Fluorescence spectra were obtained on a FluoroMax 4 luminescence spectrometer (HORIBA Jobin Yvon). UV-vis-NIR spectra were acquired by using a PerkinElmer Lambda 750 UV-vis-NIR spectrophotometer.

Cell Culture Experiments: 4T1 murine breast cancer cell line was originally obtained from American Type Culture Collection (ATCC) and cultured under recommended medium under 37 °C within 5% CO_2 atmosphere. Confocal fluorescence images were taken by a Leica SP5 confocal laser scanning microscopy. The excitation wavelengths were 488 nm for DOX and 405 nm for Ce6. Flow cytometry data was obtained by flow cytometry analysis (FACS Calibur from Becton, Dickinson and Company). The obtained data was analyzed using the FlowJo software.

Cell Toxicity Assay: 4T1 cells pre-seeded into 96-well plates (1×10^4 per well) were incubated with series concentrations of PEDOT:PSS-PEG, free DOX, free SN38, PEDOT:PSS-PEG-DOX, and PEDOT:PSS-PEG-SN38. After incubation for 48 h, the standard thiazolyl tetrazolium (MTT, Sigma-Aldrich) test was conducted to measure the relative cell viabilities compared with the untreated cells. For photodynamic therapy, 4T1 cells pre-seeded into the 96-well plates were added with series concentrations of PEDOT:PSS-PEG-Ce6 and free Ce6. After 6 h of incubation, the cells were exposed to a 660 nm laser at the power density of 0.1 W cm^{-2} for 10 min. 24 h later, the standard MTT test was conducted to measure the relative cell viabilities.

Quantitative Measurement of Ce6 and DOX Cellular Uptake: To quantitatively determine the cellular uptake of Ce6 and PEDOT:PSS-PEG-Ce6, 4T1 cells cultured in a 24-well plate (1×10^5 per well) were incubated with Ce6 or PEDOT:PSS-PEG-Ce6 at the same Ce6 concentration (2 μM). After incubation for 2 h or 6 h, the cells were washed with PBS for 3 times and then lyzed by 1 mL 2% sodium dodecyl sulfate (SDS) for 2 h to obtain homogeneous solutions, into which 1 mL 0.2 M NaOH was added to induce complete detachment of Ce6 from nanoparticles, as evidenced by the ≈100% recovery of Ce6 fluorescence in the PEDOT:PSS-PEG-Ce6 sample after treatment. Fluorescent intensities of Ce6 in the obtained solutions were measured under the excitation of 404 nm.

To quantitatively determine the cellular uptake of DOX, cells incubated with free DOX or PEDOT:PSS-PEG-DOX with or without laser irradiation were lyzed by SDS following a similar protocol as described above. A solution of hydrochloric acid-isopropanol (HCl-IPA) mixtureafter HCl-IPA treatment. Fluorescent intensities of DOX in the obtained solutions were measured under the excitation of 490 nm.

Photothermally Enhanced Chemotherapy Using PEDOT:PSS-PEG-DOX: 4T1 cells pre-seeded in 96-well plates were added with free DOX, PEDOT:PSS-PEG, or PEDOT:PSS-PEG-DOX at 0.030 mg mL^{-1} DOX equivalent concentration. The cells were then immediately irradiated by the 808 nm laser at power densities of 0.1, 0.15, and 0.2 W cm^{-2} for 20 min. After another 24 h of incubation, the standard MTT test was conducted to measure the relative cell viabilities compared with untreated cells.

Supporting Information

Supporting Information is available from the Wiley Online Library or from the author.

Acknowledgements

This work was partially supported by the National Natural Science Foundation of China (51222203, 51002100, 51132006), the National "973" Program of China (2011CB911002, 2012CB932601), and a Project Funded by the Priority Academic Program Development of Jiangsu Higher Education Institutions. Liang Cheng was supported by a Post-doctoral research program of Jiangsu Province (1202044C).

Received: May 7, 2013
Revised: June 3, 2013
Published online: June 27, 2013

[1] A. F. Hood, *Med. Clin. North Am.* **1986**, *70*, 187.
[2] T. G. Burish, D. M. Tope, *J. Pain Symptom Manage.* **1992**, *7*, 287.
[3] J. J. Monsuez, J. C. Charniot, N. Vignat, J. Y. Artigou, *Int. J. Cardiol.* **2010**, *144*, 3.
[4] O. C. Farokhzad, J. J. Cheng, B. A. Teply, I. Sherifi, S. Jon, P. W. Kantoff, J. P. Richie, R. Langer, *Proc. Natl. Acad. Sci. U.S.A.* **2006**, *103*, 6315.
[5] H. S. Yoo, T. G. Park, *J. Controlled Release* **2004**, *96*, 273.
[6] D. Goren, A. T. Horowitz, D. Tzemach, M. Tarshish, S. Zalipsky, A. Gabizon, *Clin. Cancer Res.* **2000**, *6*, 1949.
[7] H. Y. Liu, D. Chen, L. L. Li, T. L. Liu, L. F. Tan, X. L. Wu, F. Q. Tang, *Angew. Chem. Int. Edit.* **2011**, *50*, 891.

[8] B. Tian, C. Wang, S. Zhang, L. Z. Feng, Z. Liu, *ACS Nano* **2011**, *5*, 7000.
[9] X. H. Huang, I. H. El-Sayed, W. Qian, M. A. El-Sayed, *J. Am. Chem. Soc.* **2006**, *128*, 2115.
[10] W. S. Seo, J. H. Lee, X. M. Sun, Y. Suzuki, D. Mann, Z. Liu, M. Terashima, P. C. Yang, M. V. McConnell, D. G. Nishimura, H. J. Dai, *Nat. Mater.* **2006**, *5*, 971.
[11] K. Yang, S. A. Zhang, G. X. Zhang, X. M. Sun, S. T. Lee, Z. A. Liu, *Nano Lett.* **2010**, *10*, 3318.
[12] J. You, G. D. Zhang, C. Li, *ACS Nano* **2010**, *4*, 1033.
[13] H. Kang, A. C. Trondoli, G. Zhu, Y. Chen, Y.-J. Chang, H. Liu, Y.-F. Huang, X. Zhang, W. Tan, *ACS Nano* **2011**, *5*, 5094.
[14] H. Yan, C. Teh, S. Sreejith, L. Zhu, A. Kwok, W. Fang, X. Ma, N. Kim Truc, V. Korzh, Y. Zhao, *Angew. Chem. Int. Edit.* **2012**, *51*, 8373.
[15] S. P. Sherlock, S. M. Tabakman, L. Xie, H. Dai, *ACS Nano* **2011**, *5*, 1505.
[16] Y. Morimoto, M. Hirohashi, N. Kobayashi, A. Ogami, M. Horie, T. Oyabu, T. Myojo, M. Hashiba, Y. Mizuguchi, T. Kambara, B. W. Lee, E. Kuroda, M. Shimada, W. N. Wang, K. Mizuno, K. Yamamoto, K. Fujita, J. Nakanishi, I. Tanaka, *Nanotoxicology* **2012**, *6*, 766.
[17] K. Yang, J. M. Wan, S. A. Zhang, Y. J. Zhang, S. T. Lee, Z. A. Liu, *ACS Nano* **2011**, *5*, 516.
[18] E. Boisselier, D. Astruc, *Chem. Soc. Rev.* **2009**, *38*, 1759.
[19] K. Yang, L. Feng, X. Shi, Z. Liu, *Chem. Soc. Rev.* **2013**, *42*, 530.
[20] K. Yang, S. Zhang, G. Zhang, X. Sun, S.-T. Lee, Z. Liu, *Nano Lett.* **2010**, *10*, 3318.
[21] X. Liu, H. Tao, K. Yang, S. Zhang, S.-T. Lee, Z. Liu, *Biomaterials* **2011**, *32*, 144.
[22] J. Y. Chen, D. L. Wang, J. F. Xi, L. Au, A. Siekkinen, A. Warsen, Z. Y. Li, H. Zhang, Y. N. Xia, X. D. Li, *Nano Lett.* **2007**, *7*, 1318.
[23] H. Liu, D. Chen, L. Li, T. Liu, L. Tan, X. Wu, F. Tang, *Angew. Chem. Int. Edit.* **2011**, *50*, 891.
[24] S. Lal, S. E. Clare, N. J. Halas, *Acc. Chem. Res.* **2008**, *41*, 1842.
[25] G. von Maltzahn, J. H. Park, A. Agrawal, N. K. Bandaru, S. K. Das, M. J. Sailor, S. N. Bhatia, *Cancer Res.* **2009**, *69*, 3892.
[26] M. S. Yavuz, Y. Cheng, J. Chen, C. M. Cobley, Q. Zhang, M. Rycenga, J. Xie, C. Kim, K. H. Song, A. G. Schwartz, L. V. Wang, Y. Xia, *Nat. Mater.* **2009**, *8*, 935.
[27] K. Yang, L. Hu, X. Ma, S. Ye, L. Cheng, X. Shi, C. Li, Y. Li, Z. Liu, *Adv. Mater.* **2012**, *24*, 1868.
[28] S. H. Hu, Y. W. Chen, W. T. Hung, I. W. Chen, S. Y. Chen, *Adv. Mater.* **2012**, *24*, 1748.
[29] Y. S. Chen, Y. C. Hung, I. Liau, G. S. Huang, *Nanoscale Res. Lett.* **2009**, *4*, 858.
[30] N. Khlebtsov, L. Dykman, *Chem. Soc. Rev.* **2011**, *40*, 1647.
[31] K. Wang, J. Ruan, H. Song, J. L. Zhang, Y. Wo, S. W. Guo, D. X. Cui, *Nanoscale Res. Lett.* **2011**, 6.
[32] S. T. Yang, X. Wang, G. Jia, Y. Gu, T. Wang, H. Nie, C. Ge, H. Wang, Y. Liu, *Toxicol. Lett.* **2008**, *181*, 182.
[33] K. Yang, H. Xu, L. Cheng, C. Sun, J. Wang, Z. Liu, *Adv. Mater.* **2012**, *24*, 5586.
[34] Z. Zha, X. Yue, Q. Ren, Z. Dai, *Adv. Mater.* **2013**, *25*, 777.
[35] M. Chen, X. Fang, S. Tang, N. Zheng, *Chem. Commun.* **2012**, *48*, 8934.
[36] J. Yang, J. Choi, D. Bang, E. Kim, E.-K. Lim, H. Park, J.-S. Suh, K. Lee, K.-H. Yoo, E.-K. Kim, Y.-M. Huh, S. Haam, *Angew. Chem. Int. Edit.* **2011**, *50*, 441.
[37] L. Cheng, K. Yang, Q. Chen, Z. Liu, *ACS Nano* **2012**, *6*, 5605.
[38] C. Xing, Q. Xu, H. Tang, L. Liu, S. Wang, *J. Am. Chem. Soc.* **2009**, *131*, 13117.
[39] C. Zhu, L. Liu, Q. Yang, F. Lv, S. Wang, *Chem. Rev.* **2012**, *112*, 4687.
[40] X. Feng, F. Lv, L. Liu, H. Tang, C. Xing, Q. Yang, S. Wang, *ACS Appl. Mater. Interfaces* **2010**, *2*, 2429.
[41] X. Zhang, L. Meng, Q. Lu, Z. Fei, P. J. Dyson, *Biomaterials* **2009**, *30*, 6041.
[42] X. Sun, Z. Liu, K. Welsher, J. T. Robinson, A. Goodwin, S. Zaric, H. Dai, *Nano Res.* **2008**, *1*, 203.
[43] Z. Liu, J. T. Robinson, X. Sun, H. Dai, *J. Am. Chem. Soc.* **2008**, *130*, 10876.
[44] B. Y. Ouyang, C. W. Chi, F. C. Chen, Q. F. Xi, Y. Yang, *Adv. Funct. Mater.* **2005**, *15*, 203.
[45] R. R. Love, H. Leventhal, D. V. Easterling, D. R. Nerenz, *Cancer* **1989**, *63*, 604.
[46] A. Tanizawa, A. Fujimori, Y. Fujimori, Y. Pommier, *J. Natl. Cancer Inst.* **1994**, *86*, 836.
[47] T. V. Akhlynina, A. A. Rosenkranz, D. A. Jans, A. S. Sobolev, *Cancer Res.* **1995**, *55*, 1014.
[48] Z. G. Gao, A. N. Lukyanov, A. Singhal, V. P. Torchilin, *Nano Lett.* **2002**, *2*, 979.
[49] S. I. Ogura, Y. Fujita, T. Kamachi, I. Okura, *J. Porphyrins Phthalocyanines* **2001**, *5*, 486.
[50] H. Park, J. Yang, J. Lee, S. Haam, I.-H. Choi, K.-H. Yoo, *ACS Nano* **2009**, *3*, 2919.
[51] P. Wust, B. Hildebrandt, G. Sreenivasa, B. Rau, J. Gellermann, H. Riess, R. Felix, P. M. Schlag, *Lancet Oncol.* **2002**, *3*, 487.
[52] G. M. Hahn, J. Braun, I. Harkedar, *Proc. Natl. Acad. Sci. U.S.A.* **1975**, *72*, 937.